special communication

Chest wall and lung volume estimation by optical reflectance motion analysis

S. J. CALA, C. M. KENYON, G. FERRIGNO, P. CARNEVALI, A. ALIVERTI, A. PEDOTTI, P. T. MACKLEM, AND D. F. ROCHESTER
Meakins-Christie Laboratories, Montréal, Québec, Canada H2X 2P2; and Centro di Bioingegneria–Politecnico di Milano, Fondazione Don Gnocchi, 1–20148 Milano, Italy

Cala, S. J., C. M. Kenyon, G. Ferrigno, P. Carnevali, A. Aliverti, A. Pedotti, P. T. Macklem, and D. F. Rochester. Chest wall and lung volume estimation by optical reflectance motion analysis. *J. Appl. Physiol.* 81(6): 2680–2689, 1996.— Estimation of chest wall motion by surface measurements only allows one-dimensional measurements of the chest wall. We have assessed an optical reflectance system (OR), which tracks reflective markers in three dimensions (3-D) for respiratory use. We used 86 (6-mm-diameter) hemispherical reflective markers arranged circumferentially on the chest wall in seven rows between the sternal notch and the anterior superior iliac crest in two normal standing subjects. We calculated the volume of the entire chest wall and compared inspired and expired volumes with volumes obtained by spirometry. Marker positions were recorded by four TV cameras; two were 4 m in front of and two were 4 m behind the subject. The TV signals were sampled at 100 Hz and combined with grid calibration parameters on a personal computer to obtain the 3-D coordinates of the markers. Chest wall surfaces were reconstructed by triangulation through the point data, and chest wall volume was calculated. During tidal breathing and vital capacity maneuvers and during CO_2-stimulated hyperpnea, there was a very close correlation of the lung volumes (V_L) estimated by spirometry [V_L(SP)] and OR [V_L(OR)]. Regression equations of V_L(OR) (y) vs. V_L(SP) (x, BTPS in liters) for the two subjects were given by $y = 1.01x - 0.01$ ($r = 0.996$) and $y = 0.96x + 0.03$ ($r = 0.997$), and by $y = 1.04x + 0.25$ ($r = 0.97$) and $y = 0.98x + 0.14$ ($r = 0.95$) for the two maneuvers, respectively. We conclude spirometric volumes can be estimated very accurately and directly from chest wall surface markers, and we speculate that OR may be usefully applied to calculations of chest wall shape, regional volumes, and motion analysis.

chest wall motion; imaging; respiratory mechanics

EXISTING METHODS for noninvasive measurement of tidal volume (V_T) have considered V_T as the sum of changes in volume swept by the rib cage and abdomen between end expiration and end inspiration. Within limits, each of these two compartments has only a single degree of freedom, so that when appropriately calibrated, measurement of the motion of the two parts can be converted to the volumes swept by them, which, when summed, give V_T. Current techniques, utilizing linearized magnetometry to measure distance or inductance plethysmography to measure cross-sectional area and estimate V_T, ignore small but systematic distortions of the rib cage. Recently, the rib cage has been considered as a two-compartment system, the lung-apposed or pulmonary rib cage and the diaphragm-apposed or abdominal rib cage (1, 5, 19). The validity of the calibration coefficients obtained experimentally to convert one or two dimensions to volume is limited to the estimation of V_T under conditions matched to those during which the calibration was performed. Other investigators have reported the errors introduced by their application to other conditions (4, 13, 18, 20). In addition, particularly in a clinical setting, adequate calibration data may be difficult to obtain because of poor subject cooperation.

Alternatively, as discussed by Konno and Mead (11), a geometric technique could be used to describe the relationship between the volume contained by the parts of the chest wall and to calculate their respective volume changes. This approach has the potential to dispense with calibration factors and could therefore be free of any associated errors. Noninvasive three-dimensional (3-D) techniques have already been employed to obtain measurements of V_T directly, although each has particular limitations. The 3-D X-ray-computed tomography, using the Dynamic Spatial Reconstructor (12), is capable of measuring a known volume to within 2% and has adequate temporal resolution to provide dynamic images of the chest wall during respiratory movements. However, it requires high doses of ionizing radiation, is limited to the supine posture, and is unsuitable for long analyses. Optical systems based on sculptured light (16) have low temporal resolution, require time-consuming data processing, and are unavailable for routine use. Technical developments in image processing and parallel computing have enabled the analysis of the movements of multiple points on the body surface to be performed using an optical reflectance motion-analysis system (OR; 2, 3, 6, 10). The television image processor, known as ELITE (ELaboratore di Immagini TElevisive; Milan Polytechnic, Milan, Italy), OR is a digitized vision system designed to identify objects of a predetermined shape and to monitor their trajectories in 3-D and in real time. It has been used extensively as an automatic movement analyzer in biomechanics and in orthopedic and neurological medicine (6, 9, 15). Recently, OR was adapted to estimate directly the volume change of the chest wall

during respiration by computing the 3-D coordinates of 32 markers placed on the rib cage and abdomen (7). A geometric model based on 54 tetrahedrons was used for computation of volume in which the chest wall between the second rib and umbilicus was measured as upper rib cage, lower rib cage, and abdomen. Although the correlation coefficient of the relationship between spirometrically (SP) obtained lung volume (V_L) [V_L(SP)] and that computed by the model was high (0.98), V_L calculated by OR [V_L(OR)] was substantially less than V_L(SP) (13.3% error ATPS; 21.3% error BTPS). This difference clearly limited the ability of OR to predict V_L directly, because a calibration factor was still required.

In this study, we report the use of OR to estimate the change in V_L (ΔV_L), using more extended boundaries of the chest wall than those reported by Ferrigno et al. (7). We hypothesized that a direct estimate of ΔV_L based on changes in chest wall volume required circumferential measurements of chest wall displacement between the thoracic inlet and the pelvis. In the study by Ferrigno et al. (7), the portion of the abdominal compartment caudal to the umbilicus, the rib cage cranial to the second rib, and the chest wall in the axillary region were not included in the imaging field. Hence the underestimate of V_L in the study by Ferrigno et al. (7) was likely to be because a substantial fraction of V_L resulted in displacement of the chest wall beyond the boundaries used in their analysis. A prediction arising from our hypothesis was that the accuracy of V_L(OR) could be improved if the number of markers were increased to include these regions. Therefore, the main difference between this study and that of Ferrigno et al. (7) is that we have utilized almost three times the number of markers to create a much larger marker array, arranged in a circumferential rather than cubic configuration. We further anticipated that by calculating the relationship between the error in ΔV_L(OR) and the number of markers utilized in the analysis we would be able to quantify the minimum number of markers required to achieve a given level of accuracy. Finally, we aimed to test the hypothesis that chest wall shape could be estimated by a simple geometrical model.

METHODS

OR

The components of the OR have been described in detail previously (3, 6, 8). Briefly, small (6 mm), lightweight, hemispherical markers were attached to the subject with double-sided adhesive tape and observed with the use of two infrared (IR) charge-coupled device (CCD) cameras. The cameras are placed 4 m behind and 4 m in front of the subject. It is important for this distance to be maintained so that the markers do not change size significantly, as viewed by the cameras. For respiratory use, there is a defined "safe zone" $1.5 \times 1.5 \times 1.5$ m that the subject should stay within to maintain system calibration. This is an easy requirement to fulfill in standard exercise protocols involving cycle ergometry or treadmill exercise. The cameras were of the CCD solid-state type and were fitted with zoom lenses that allow the best definition in the images over the 4-m distance to the subject at a sampling frequency of up to 100 Hz. The cameras use a lighting system consisting of a circular ring of IR light-emitting diodes (LEDs) coaxial with the lenses and strobe lighted to obtain sharp pictures without comet-tail effect. IR strobes were used for image acquisition to freeze images sharply. Markers were identified with hardware pattern recognition, and the marker centroids were calculated from each camera image and then stored. Stereophotogrammetric techniques combined centroids from individual camera images to obtain 3-D coordinates on an IBM-compatible personal computer (PC) in a postacquisition software step. Data can be acquired at up to 100 Hz, and the system has an accuracy of 1/20,000 of the field of view, ~0.2 mm in each spatial coordinate, as used for respiratory maneuvers (17).

Sensor Placement

We used 86 IR-reflective markers in a configuration shown in Fig. 1. The grid system consisted of seven horizontal rows arranged circumferentially between the level of the clavicles and the anterior superior iliac spine. Along the horizontal rows, the markers were arranged anteriorly and posteriorly in five vertical columns, and there was an additional bilateral column in the midaxillary line. The anatomical landmarks for the horizontal rows were, craniocaudally, *1*) the clavicular line; *2*) the manubrio-sternal joint (adjacent to the 2nd rib); *3*) the nipples (~5th rib); *4*) the xiphoid process [approximately the top of the area of apposition of the diaphragm to the rib cage at functional residual capacity (FRC) in the upright posture, confirmed by percussion]; *5*) the lower costal margin (10th rib in midaxillary line); *6*) umbilicus; and *7*) anterior superior iliac spine. Along the horizontal rows, the markers were placed in the following positions: *1*) the midlines (anteriorly, along the sternum and continuing caudally below the xiphoid through the umbilicus, and posteriorly, along the spinous processes of the vertebral column); *2*) both anterior and posterior axillary lines; *3*) the midpoint of the interval between the midline and the anterior axillary line (just medial to the nipple line) and the midpoint of the interval between the midline and the posterior axillary line; and *4*) the midaxillary lines.

To provide better detail of the costal margin, we included an extra marker bilaterally at the midpoint between the xiphoid and the most lateral portion of the 10th rib; to increase marker density in regions where the markers were well separated, we added two markers in the region overlying the lung-apposed rib cage and two markers in the corresponding posterior positions.

Consequently, there were 42 anterior markers, 34 posterior markers, and 10 lateral markers. With the exception of the midaxillary positions, all markers were attached to the skin with double-sided adhesive tape. Because the midaxillary markers were not visible to the cameras side on, they were mounted on rear-facing right-angle brackets, before being attached to the skin.

Experimental Setup

The experimental setup is shown schematically in Fig. 2. Two IR CCD cameras were positioned 4 m in front of, and two were 4 m behind, the subject. Each pair of cameras was arranged vertically. The bottommost was at waist height and parallel to the floor; the camera ~1.5 m above was inclined downward. The subject stood with hands on the waist in the center of a space where the calibration routine for the image processor had previously been carried out. This allowed direct visualization of the anterior and posterior markers by their respective cameras. The calibration involved calculating the 3-D position of an array of sensors whose alignment on the grid was already known.

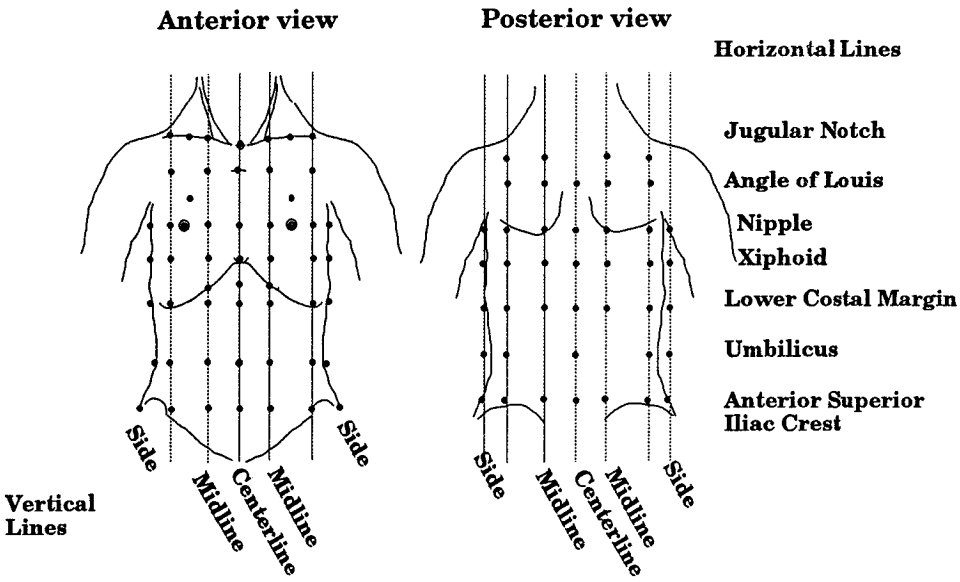

Fig. 1. Placement of infrared (IR) reflective markers on the chest wall: 42 anterior, 34 posterior, and 10 lateral between clavicles and anterior superior iliac crest for erect subjects. There were 7 circumferential horizontal rows between the clavicles and the anterior superior iliac spine and 5 vertical columns anterior and posterior, with an additional column bilateral in the midaxillary line. Surface landmarks for the horizontal rows were, craniocaudally, *1*) the clavicular line; *2*) the manubrio-sternal joint (angle of Louis); *3*) the nipples; *4*) the xiphoid process; *5*) the lower costal margin; *6*) umbilicus; and *7*) anterior superior iliac crest. Surface landmarks for the vertical columns were *1*) the midlines; *2*) both anterior and posterior axillary lines; *3*) the midpoint of the interval between the midline and the anterior axillary line and the midpoint of the interval between the midline and the posterior axillary line; and *4*) the midaxillary lines. Extra markers were added bilaterally at the midpoint between the xiphoid and the most lateral portion of the 10th rib, in the region overlying the lung-apposed rib cage, and in corresponding posterior positions.

The subject breathed on a mouthpiece connected to a 9-liter water-displacement spirometer (Warren Collins) containing room air. For rebreathing experiments, the soda lime absorber was removed. The spirometer had been checked for leaks and calibrated before the experiment, using a set of syringes ranging from 1 to 5 liters, and was fitted with a potentiometer, the analog output of which was transmitted via an analog-to-digital (A-to-D) board to the computer.

Experimental Protocol

We studied two normal male subjects (S1 and S2, ages 27 and 36 yr). One (S1) was experienced in respiratory maneuvers. Subjects had vital capacities (VC) of 5.2 and 5.1 liters, respectively. During the experiment, the subjects carried out a number of ventilatory maneuvers. Initially, after a period of quiet breathing, they performed three slow VC maneuvers. Next, after closing the glottis, they performed belly-in, belly-out isovolume maneuvers at residual volume (RV), ~50% expiratory reserve volume (ERV), FRC, end of tidal breath, ~50% inspiratory capacity (IC), and total lung capacity (TLC). Then, by removing the CO_2 absorber and allowing the CO_2 to accumulate within the spirometer, they performed a CO_2-induced hyperpnea lasting ~3 min and terminated when the V_T was ~100% greater than baseline. Baseline drift of the spirometer due to O_2 consumption ($\dot{V}O_2$) in the first maneuver was corrected for by comparing FRC levels at the beginning and end of the recording and adjusting for the slope. Spirometer drift in the second experiment was more complicated because the subjects were not in a steady state and the respiratory exchange ratio was not unity. Thus we took the difference between the spirometer and the OR measurements at end expiration at the end of the run (only) and corrected for an (assumed) constant slope. Finally, to assess the effect of change in truncal posture at isovolume of lung ($V_{L_{iso}}$) on the estimation of chest wall volume by OR, the subjects performed two additional maneuvers after closing the glottis at relaxed FRC with both hands placed on the waist. First, they flexed the trunk laterally from the waist to ~15° from the vertical, held the posture briefly, and then returned to the original position. Second, they elevated the shoulder girdle by 4–5 cm, held the position constant, and returned to baseline again.

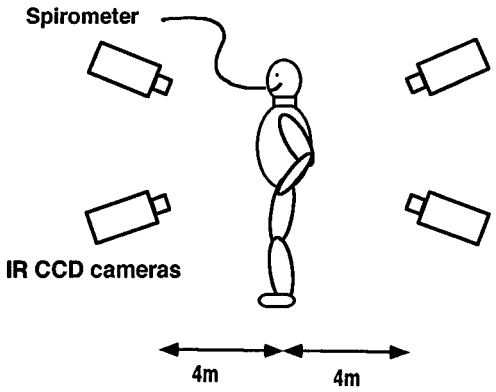

Fig. 2. Experimental setup of IR charge-coupled device (CCD) camera positions and subject position. Camera output goes via special-purpose hardware to an IBM-compatible personal computer (PC; not shown).

Volume Calculation

Volume displacement of the chest wall was calculated by triangulating the surface and integrating the subtended volume. The actual triangulation used is shown in Fig. 3. Note that additional "virtual" points were constructed at

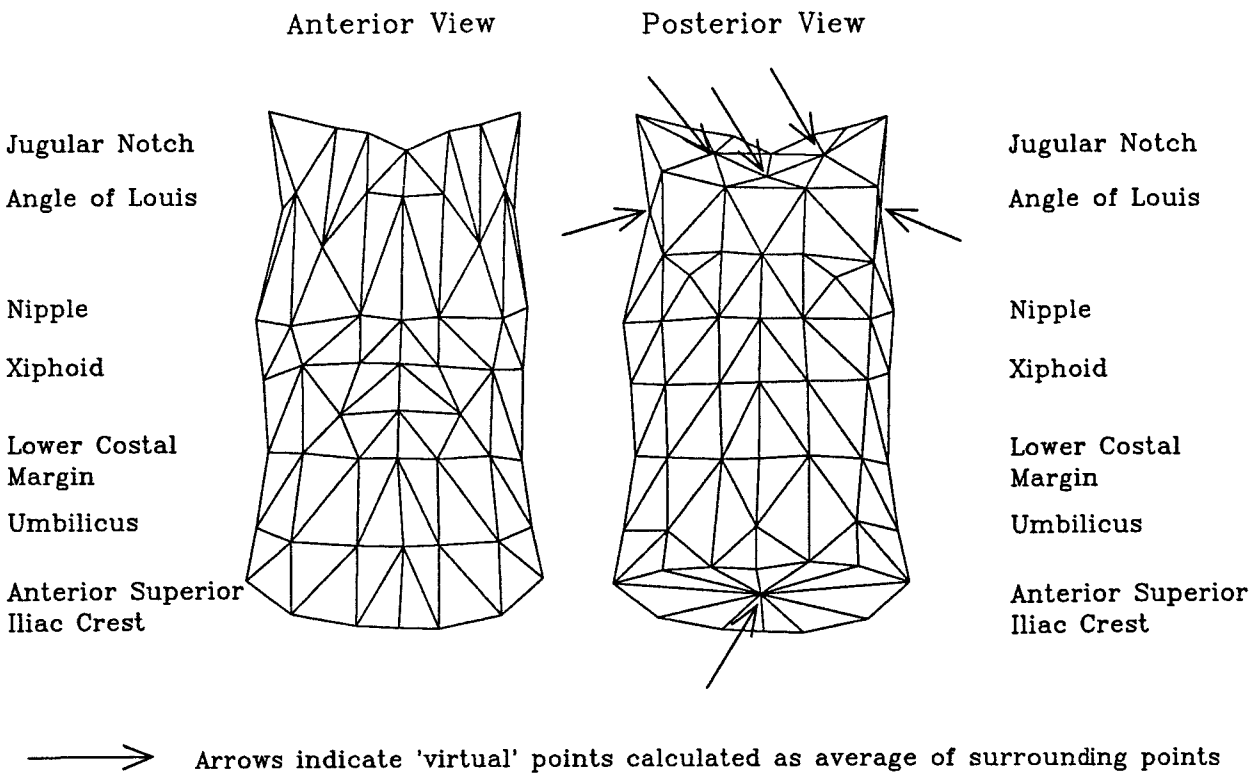

Fig. 3. Surface triangulation used for volume calculations. Points indicated by arrows were automatically constructed from surrounding points to enable simple triangulation over regions where no points could be placed, e.g., at center of the body to construct the lower boundary.

various margins to enable easier triangulation. For example, a point was constructed at the mean position of all the points on the anterior superior iliac spine level. Similar virtual point construction and triangulation allow completely arbitrary subdivision of the chest wall. In particular, the detail points on the lower costal margin are useful for division of the chest wall into anatomic compartments.

The steps involved in the calculation are as follows. Having defined an arbitrary 3-D (x, y, z) coordinate system, we found it possible to define the x, y, and z coordinates of each marker, the area (A_i), the x, y, z coordinates of the centroid, and the distance (d_i) of each triangle i to an arbitrary reference plane. From the direction of the normal to each triangle i, the angle of the plane defined by that triangle with respect to the reference plane (q_i) can be determined. Each triangle is then used to define a volume element (V_i) with respect to an arbitrary reference plane where $V_i = A_i \cdot d_i \cdot \cos q_i$. The term $\cos q_i$ will be positive for the triangles, the outer faces of which are away from the reference plane and negative for those pointing toward it. Total volume (V) of the thorax enclosed within the surface defined by these triangles is given by the summation of all volume elements, i.e., $V = \Sigma_i V_i$. This procedure is equivalent to the Gauss theorem. It is important to note that it was not possible to calculate absolute V_L by using OR. All estimates of V_L(OR) were therefore calculated as the difference between estimates of chest wall volume, which could then be compared with the spirometric equivalent. For statistical comparisons of the change in V_L(SP) vs. V_L(OR), we calculated the mean difference and divided by the SD to obtain the coefficient of variation. We defined accuracy as the coefficient of variation for the maneuvers studied where this was applicable and unless otherwise stated.

Sensitivity Analysis

To determine the dependence of the regression analysis on the number of points, we systematically removed horizontal and vertical rows of points in the volume calculation and recalculated the regression analysis. Horizontal rows were removed both singly and in adjacent pairs, and vertical rows were removed singly. Because we calculated chest wall volume by triangulation between adjacent points, combinations of nonadjacent row removals were simply additive in terms of effect. We also assessed the effect of removing the extra "detail" points.

To investigate the theoretical connection between the number of points and expected accuracy, we modeled the cross section of the chest wall using an "athletic track" shape (two semicircles separated by a rectangle). By varying the number of points on the curved regions we could obtain a theoretical limit on the possible accuracy of any number of points on a particular space along its arc ($n > 2$); then the area enclosed by the polygon P that they form is

$$P = (n - 1) * r^2 * \sin [\Pi/(n - 1)] \quad (1)$$

where r is the radius of the semicircle. Thus the percentage difference from the true cross-sectional area consisting of both semicircles and the rectangle in the center is

$$\text{Error } (\%) = (\Pi * r^2 - 2\Pi)/[(\Pi * r^2) + (2r * s)] \quad (2)$$

where s is the distance between the two semicircles. This will always be an underestimate. Assuming that there is much less curvature vertically on the chest wall than on a horizontal cross section, this translates immediately into a limit on the volume accuracy. We calculated this expected error for

both subjects from their chest wall dimensions and the number of markers used on a horizontal level.

Finally, an important issue is the time required by the operator(s) to calibrate the equipment, attach markers to the subject, and analyze the data. To minimize operator time, a number of automated routines have been incorporated into the calibration, data processing, and data reduction phases. First, the space occupied by the subject is calibrated before the experiment, using a square pegboard array consisting of a grid of markers having the same dimensions as those to be used in the study at a known constant distance from one another. This is imaged by the system, and the calibration is performed automatically by the software in seconds without operator intervention beyond specifying which calibration grid is to be used. The algorithm contained in the software has been previously described (2). Calibration involves two persons and takes ~15 min to set up and perform. The 86 markers are attached manually, in 30–45 min, depending on the speed and accuracy of the operator in locating the anatomical landmarks, but as noted, it is not necessary to recalibrate afterwards. Finally, the data-reduction stage has been considerably streamlined to minimize operator time, using a two-level architecture incorporating a number of automated calculations. The final level of calculations, namely volume estimation, can easily be performed by a PC rather than workstation. The most time-consuming step in volume estimation (2–3 min) is manual labeling of each of the 86 markers in the first frame of each sequence. Henceforth, remaining steps are highly automated. The hardware processor analyzes the images in real time. Then, using a technique based on a convolution operator, the processor recognizes within each frame objects having a specific shape. The coordinates of the markers are fed into the computer, and marker trajectories are then tracked automatically.

RESULTS

Isovolume Maneuvers

V_L(OR) during isovolume maneuvers over the VC is shown for the two subjects in Fig. 4. In S2, the amplitude of oscillations during the isovolume maneuver was consistently <250 ml, irrespective of V_L. At TLC, there was a ~600 ml decrease in V_L(OR) over the first ~5 s before a stable value was attained. Conversely, the V_L(OR) baseline increased by ~300 ml for the first ~5 s at RV before reaching stability. In S1, the fluctuations in V_L(OR) during the isovolume maneuver were larger, especially at V_L above FRC, with a comparable downward drift in the V_L(OR) baseline at TLC.

Comparison of OR with Spirometer

Quiet breathing and VC maneuvers. Figure 5 shows a representative example of a VC breath bracketed by tidal breathing in S1 and S2, comparing estimates of V_L(OR) and V_L(SP) and regressions of V_L(OR) vs. V_L(SP) corresponding to the same data. The regression equations relating V_L(OR) to V_L(SP) for S1 and S2 are $V_L(OR) = 1.04\ V_L(SP) + 0.02$ ($r = 0.995$) and $V_L(OR) = 0.99\ V_L(SP) - 0.01$ ($r = 0.995$), respectively. Analysis of the residual error from the regression of V_L(OR) vs. V_L(SP) revealed that 96% of the points were within 250 ml of the regression line in both subjects and that the coefficient of variation was 1.9 and 2.3% for S1 and S2, respectively.

Involuntary CO_2-Stimulated Hyperpnea

Figure 6 shows representative data from the first and last 30 s of CO_2-induced hyperpnea, comparing V_L(OR) and V_L(SP) results for S1 and S2 and regressions of V_L(OR) vs. V_L(SP) corresponding to the same data. The regression equations for S1 and S2 were $V_L(OR) = 1.00\ V_L(SP) - 0.05$ ($r = 0.97$) and $V_L(OR) = 0.99\ V_L(SP) - 0.04$ ($r = 0.97$), respectively. The coefficient of variation of the residual error was 3.6 and 4.4% for S1 and S2, respectively, and 96% of the points were within 350 ml of the regression line.

Sensitivity Analysis

Marker number. The effect of marker removal on the slope of the relationship between V_L(OR) and V_L(SP) was dependent on both the maneuver and the subject (Fig. 7). Chest wall volume estimation was more sensitive to marker removal during hyperpnea maneuvers than during simple quiet breathing and VC. For the removal of vertical lines of markers, there was always an increase in the slope of between 3 and 10% for the midlines on the back (S2) and the side markers (S1). A combination of side and midline markers resulted in increases of slope from 5% (S2) to 20% (S1). The effect of horizontal line removal was most important at the clavicular and anterior superior iliac spine levels in

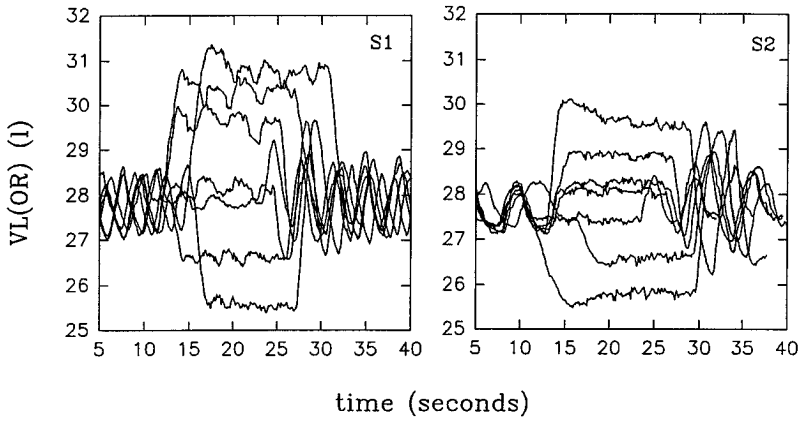

Fig. 4. Isovolume maneuvers in *subject 1* (S1) and *subject 2* (S2) at residual volume, ~50% expiratory reserve volume, functional respiratory capacity, end of tidal breath, ~50% inspiratory capacity (IC), 75% IC, and total lung capacity. Maneuvers were bracketed by quiet tidal breathing. V_L(OR), lung volume (optical reflectance system).

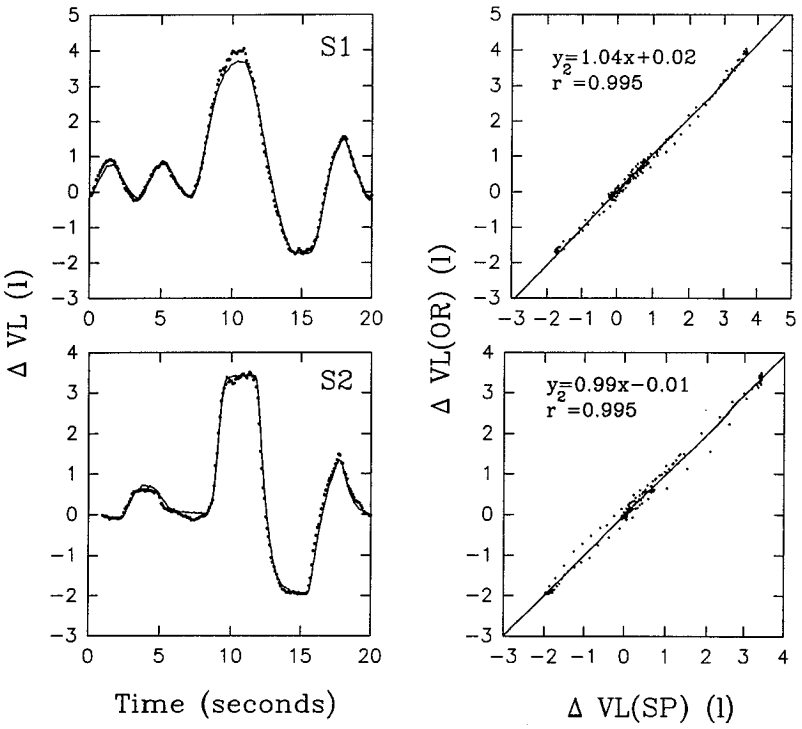

Fig. 5. Representative example of tidal breathing and vital capacity (VC) breath in S1 and S2, comparing estimates of change in VL (ΔVL) by spirometry (SP) and OR (*left*) and regressions of ΔVL by SP vs. OR corresponding to same data (*right*).

both subjects and maneuvers, and at the lower costal margin level for S1, leading to an increase in slope by ~10%. The intercepts of the regression lines were fairly insensitive to the removal of vertical or horizontal lines of marker with a range of changes of only 0.2 liters.

Posture. The effect of posture on the accuracy of VL(OR) is shown in Fig. 8. When the glottis was closed at FRC and the subject performed a slight lateral flexion maneuver of the trunk to ± 10°, there was no systematic effect on VL(OR). In contrast, there was a substantial (~700 ml) apparent increase in VL(OR) when the subject elevated the shoulders by ~4 cm at closed-glottis FRC.

Cross-sectional area. The error in cross-sectional area was calculated from the athletic track model of two semicircles separated by a rectangle (Fig. 9). The semicircle describes the lateral portion of the chest wall

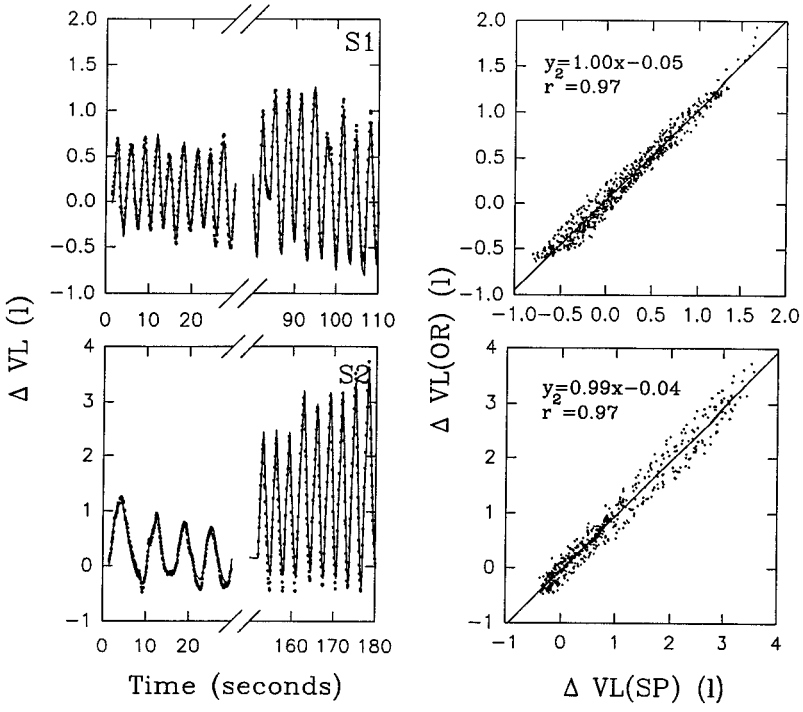

Fig. 6. Representative data from first and last 30 s of CO_2-induced hyperpnea, comparing SP and OR results for the 2 subjects (*left*) and regressions of ΔVL by SP vs. OR corresponding to same data (*right*).

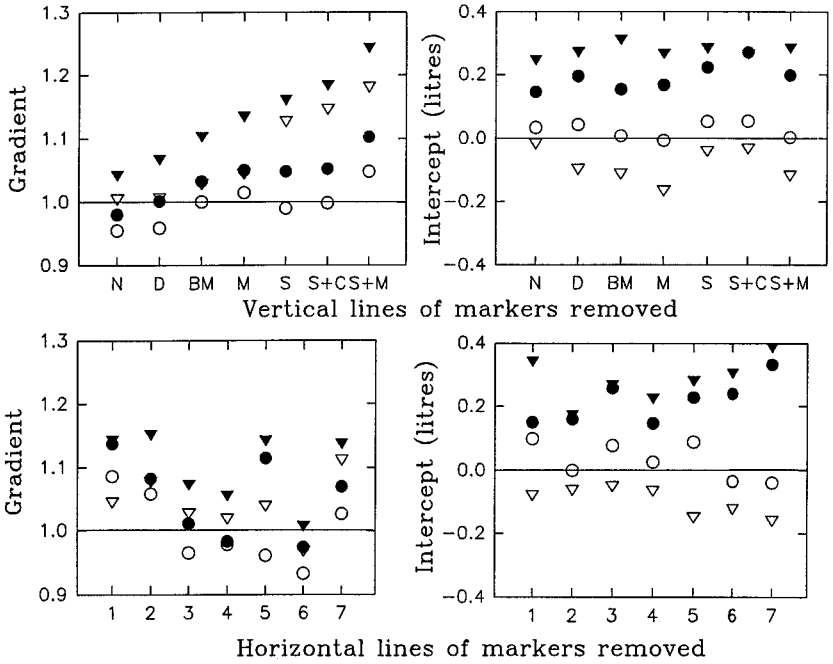

Fig. 7. Effect of marker density on slope and intercept of regression relationships between OR and SP estimates of ΔV_L. Inverted triangles, S1; circles, S2; open symbols, quiet breathing and VC maneuvers; filled symbols, CO_2-induced hyperpnea; r values >0.93 and $P < 0.001$ in all cases. *Top*: vertical lines of markers removed were N, none; D, detail markers; BM, back midlines; M, midlines; S, sides; S+C, sides and centerlines; S+M, sides and midlines. *Bottom*: horizontal lines of markers removed: 1, jugular notch; 2, angle of Louis; 3, nipple; 4, xiphoid; 5, lower costal margin; 6, umbilicus; 7, anterior superior iliac crest.

bounded medially by a sagittal plane located halfway between the nipple line and the midline. The percent error is inversely related to the number of markers on a semicircle going from >30% underestimate with three markers to ~10% with five markers to >5% with seven markers. We used 12 markers on each horizontal cross section, with five markers on each semicircle. Given the anteroposterior and transverse diameters of the two subjects, the area of the central rectangle ranged from 22% at RV to 26% at TLC. Although the relative dimensions of these central rectangular sections are not equal, we have neglected the small differences in their relative dimensions because they have the same shape. Thus we expect a cross-sectional error of $-10\% \times (100 - 22)/100$ to $-10\% \times (100 - 26)/100$, i.e., -7 to -8%, or gradients of 0.92 to 0.93, because this model is realistic and error in cross-sectional area translates directly into volume error.

DISCUSSION

With the use of an optical system to image 86 markers arranged circumferentially between the clavicles and the anterior superior iliac crest, it was possible to estimate V_L directly with a coefficient of variation of <2% for V_L, <3.5% for ΔV_L, and <1% for chest wall volume. This was a substantial improvement compared with the previous method (~21% error, BTPS), was obtained without a calibration correction factor, and applied to the entire VC range under static and dynamic conditions. When marker density was decreased, the error in estimating V_L increased markedly on removal of the cranial and caudal horizontals and, to a lesser extent, for the markers in the axillae. Assuming an athletic track model for chest wall cross-sectional shape, there was a hyperbolic relationship between error in V_L and marker number. When the

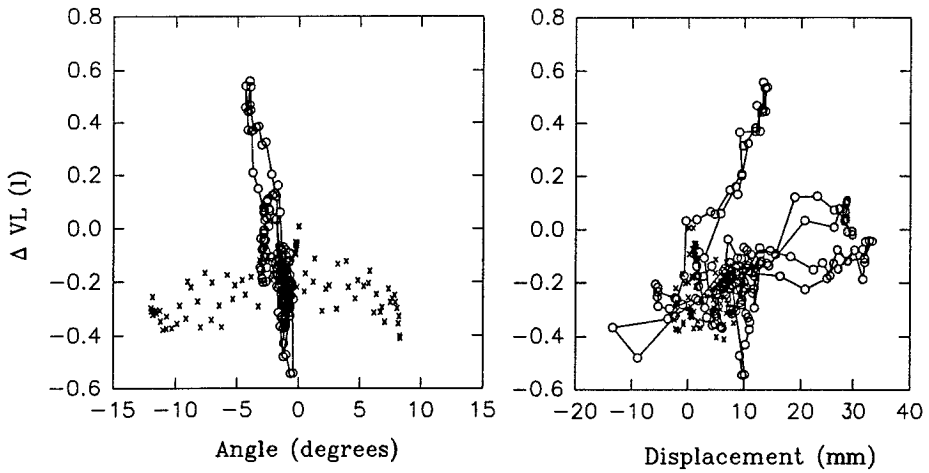

Fig. 8. Typical effect of posture on V_L(OR) during closed glottis, leaning from side to side (x) and shoulder elevations (o).

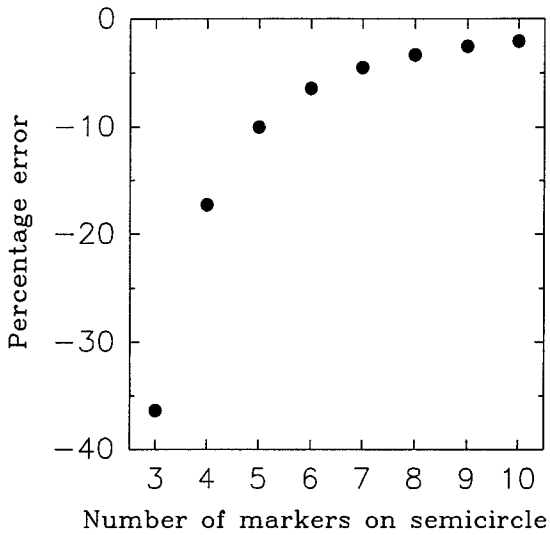

Fig. 9. Theoretical analysis of the error in calculating true chest wall cross-sectional area of the lateral chest wall by using a polygonal model. Correct shape at any given level was assumed to be a semicircle. Error in calculating area of each semicircle is a function of the no. of triangles, and therefore surface markers, used. Predicted error is plotted against no. of markers on a semicircle. Note the predicted error (~10% for 5 markers, as used in this study) is substantially greater than observed.

error prediction for a given cross section was extrapolated to the entire chest wall, the predicted error (7–8%) was somewhat larger than the range observed in this study.

Critique of Methods

Measurement errors of SP. Potential sources of error in V_L(SP) during prolonged breathing include those due to gas leakage and temperature elevation within the system, thus causing spurious increases and decreases in measured V_L, respectively. In non-steady-state breathing, especially as in our second experiment when the soda lime absorber was removed, the volume ratio between CO_2 elimination and $\dot{V}O_2$ becomes important and would presumably have been diminished, because the mixture breathed would decrease CO_2 elimination. When a weight was added to the sealed system, the deflection in the volume baseline was <25 ml/min. Although gas temperature within the drum was not measured, the length of tubing interposed between the subject and spirometer was ~2 m, so that heat loss from the tube should have dissipated most of the heat of the expired water vapor, thus minimizing temperature change within the system. Offline, to facilitate comparison of the two estimates of V_L, the $\dot{V}O_2$ slope was calculated and assumed as a constant to correct the end expiratory baseline values. In the rebreathing runs, the difference between the two estimates of V_L at the end of the run was used to correct the spirometric drift. There was a systematic increase in spirometric volumes of about 0.4 l/min, probably due to a decrease in CO_2 consumption and an increase in $\dot{V}O_2$ by ~150–200 ml/min above a hypothetical baseline value for $\dot{V}O_2$ of ~250–300 ml/min. Because the subjects were standing rather than seated, $\dot{V}O_2$ at rest and during hyperpnea may have increased because of energy consumption by postural muscles.

Changes in chest wall volume not due to gas movement. We assumed that the only factor causing chest wall volume changes was gas movement. However, lung gas volume would be affected by changes in alveolar pressure from FRC to TLC relaxed with glottis closed of probably ~30 cmH_2O (0 to ~30 cmH_2O), which, at normal atmospheric pressure (~1,000 cmH_2O), would give a 3% decrease in gas volume from active TLC with glottis open to fully relaxed with glottis closed. Alternatively, RV to FRC alveolar pressure changes during relaxation by ~20 cmH_2O (−20 to 0 cmH_2O), suggesting increases of ~2%. We observed a consistent decrease in V_L during isovolume maneuvers at TLC of ~0.5 liter, which for the two subjects was ~6% (Fig. 4). Below FRC, there were consistent increases in volume only in S1 of ~5%. However, relaxation at RV is difficult, and only S1 was highly trained in respiratory maneuvers. Ventilation is accompanied by flux of blood into and out of the thorax from the head, abdomen, pelvis, and legs. The magnitude of the respiratory-related blood volume shifts is determined by two factors. The first is the effect of pleural pressure swings on beat-to-beat variation in cardiac output. During inspiration, venous return is increased slightly, and cardiac output decreased slightly. The reverse process occurs during expiration. Flux of blood volume across the upper and lower chest wall boundaries may lead to a slight overestimate at end inspiration and a slight underestimate at end expiration of change in chest wall volume estimated by OR compared with V_L(SP) and therefore to a spuriously high V_L(OR). During isovolume maneuvers, the shifts may be somewhat larger. This may account for the rest of the error in the changes in V_L(OR) during isovolume maneuvers above lung gas pressure changes. The second process, occurring over the course of the study, is progressive blood pooling in the lower limbs, which may be seen as a gradually increasing underestimate of V_L(OR) compared with V_L(SP). However, blood pooling is not appreciable for several hours, whereas each of the observations in these studies was concluded within 10 min.

Measurement errors of OR volume of chest wall. The error in the calculation of the marker centroid coordinates by OR in 3-D has been reported previously for static and dynamic conditions to be <0.2 mm for the size of field of view used for thoracic imaging, a 1.5 m cube (17).

The volume calculation model is that of an irregular polyhedron, containing the chest wall and having flat triangular faces with vertices at the reflective markers. The volume here is directly calculated from a geometric model rather than by measuring movements of individual parts which have an assumed fixed relation to total volume changes calculated via a calibration process. Theoretically, this is superior in that the range of validity of the calculated volume changes may be much greater and also no calibration factor is required. Although we observed marker movements of 1–2 cm relative to lower rib positions during large breaths,

marker movement at the clavicular and anterior superior iliac crest was almost absent (<2 mm), translating into only 100–300 ml of volume change.

Clearly, a polyhedron model is only an approximation to the curved surface of the chest wall, but our experiments indicate a very high accuracy, with an acceptable error of <3.5% for changes in V_L. However, this accuracy is greater than the theoretical limit, based on an athletic track model of chest wall cross section (7–8%, Fig. 9). We hypothesize this is because the cross section of the chest wall is less curved than the athletic track model. In particular, the back is flatter, as are the sides of the rib cage and abdomen. This suggests markers should be positioned on chest wall "corners," because these are well defined. This also implies that refining the volume calculation model by using a curved rather than a flat approximation for the surface is inappropriate.

Sensitivity of V_L calculation to number of markers. The slope of the relationship between V_L by the optical and spirometric methods was markedly, but nonsystematically, influenced by the progressive deletion of markers, in particular horizontal and vertical lines (Fig. 7). The greatest changes, of ~10%, in both subjects resulted from removing horizontal rows of markers at the clavicles or the anterior superior iliac crest. Furthermore, in one subject (S1), the removal of the vertical lines of side markers also gave a large error (10%). This was probably because of a more rounded chest wall shape than in S2. The intercept of the regression relationships was relatively insensitive to any changes, probably because all of the points were either within a moving "part" or very close to its anatomical boundary, so that no significant volume could be included or removed by removing markers.

In light of these results, an important contribution to the error in the study by Ferrigno et al. (7) was the model used for V_L estimation. The results suggest that the explanation for the ~20% error obtained previously in estimating V_L was due to an approximately equal contribution of neglect of abdominal volume below the umbilicus (10%) and lack of side markers (~10%). Therefore, when calculating the minimum number of markers required to obtain reasonable accuracy of estimating V_L (<10%), it is evident that the detail markers and those at the xiphoid and umbilical horizontal levels are clearly expendable, saving 28 markers and leaving 58.

In summary, using an OR to calculate the volume of the chest wall during respiration over the VC in two normal standing subjects, we obtained a very high level of agreement between the calculated change in V_L and SP. The results of V_L estimation by the optical method were obtained directly, without requiring a calibration factor. Systematic elimination of markers from the volume algorithm showed that the accuracy of the calculations was critically dependent on inclusion of data from the cranio-caudal and lateral extremities of the chest wall. In addition, with the assumption of an athletic track model of the chest wall in cross section, a minimum of ten markers is required for an estimate of cross-sectional area within 5%.

The system has the advantage of suitability for use in unconstrained subjects breathing without a mouthpiece and has particular advantages in patient and/or pediatric studies where cooperation may be difficult to obtain. Once the sensors have been applied, no additional time costs are incurred during the experiment, and the on-line data processing makes it possible to analyze the very large data sets quickly and with relatively modest data storage requirements. The chest wall reconstruction computations are simple and easily modified to accommodate a greater or lesser number of markers. Because the chest wall can be imaged directly in 3-D, the data is amenable to a wide range of analyses, such as statistical analysis of chest wall coordination (10) and estimation of chest wall compartment volumes (7).

This work was supported by the Allen and Hanburys Thoracic Society of Australia and New Zealand Fellowship, the J. T. Costello Memorial Research Fund, the Medical Research Council of Canada, Respiratory Health Network of Centres of Excellence (Canada), Pro Juventute Don Carlo Gnocchi Foundation, and TELETHON Italia.

Address for reprint requests: P. T. Macklem, Montreal Chest Hospital Centre, 3650 St. Urbain, Montreal, Quebec, Canada H2X 2P4.

Received 3 October 1995; accepted in final form 7 August 1996.

REFERENCES

1. **Agostoni, E., and E. D'Angelo.** Statics of the chest wall. In: *The Thorax*, edited by C. Roussos and P. T. Macklem. New York: Dekker, 1988, vol. 29, pt. A, p. 259–295. (Lung Biol. Health Dis. Ser.)
2. **Borghese, N. A., and G. Ferrigno.** An algorithm for 3-D automatic movement detection by means of standard TV cameras. *IEEE Trans. Biomed. Eng.* 32: 1221–1225, 1990.
3. **Carnevali, P., G. Ferrigno, A. Aliverti, and A. Pedotti.** A new method for 3-D optical analysis of chest wall motion. *Technol. Health Care* 4: 43–65, 1996.
4. **Cramer, D., A. Peacock, and D. Denison.** Temperature corrections in routine spirometry. *Thorax* 39: 771–774, 1984.
5. **Decramer, M., A. De Troyer, S. Kelly, L. Zocchi, and P. T. Macklem.** Regional differences in abdominal pressure swings in dogs. *J. Appl. Physiol.* 56: 1682–1687, 1984.
6. **Ferrigno, G., N. A. Borghese, and A. Pedotti.** Pattern recognition in 3-D motion analysis. *ISPRS J. Photogramm. Remote Sens.* 45: 227–246, 1990.
7. **Ferrigno, G., P. Carnevali, A. Aliverti, F. Molteni, G. Beulke, and A. Pedotti.** Three-dimensional optical analysis of chest wall motion. *J. Appl. Physiol.* 77: 1224–1231, 1994.
8. **Ferrigno, G., and A. Pedotti.** ELITE: a digital dedicated hardware system for movement analysis via real-time TV signal processing. *IEEE Trans. Biomed. Eng.* 32: 943–950, 1985.
9. **Frigo, C.** Three-dimensional model for studying the dynamic loads on the spine during lifting. *Clin. Biomech.* 5: 143–152, 1990.
10. **Kenyon, C. M., R. H. Ghezzo, S. J. Cala, G. Ferrigno, A. Pedotti, P. T. Macklem, and D. F. Rochester.** Statistical methods for analysis of coordination of chest wall motion using optical reflectance imaging of multiple markers. In: *Mathematical Methods in Medical Imaging III. Proceedings of the Society for Optical Engineering*, edited by F. L. Bookstein, J. S. Duncan, N. Lange, and D. C. Wilson. San Diego, CA: 25–26 July 1994, p. 169–179.
11. **Konno, K., and J. Mead.** Measurement of the separate volume changes of rib cage and abdomen during breathing. *J. Appl. Physiol.* 22: 407–422, 1967.
12. **Krayer, S., K. Rehder, K. C. Beck, P. D. Cameron, E. P. Didier, and E. A. Hoffman.** Quantification of thoracic volumes

by three-dimensional imaging. *J. Appl. Physiol.* 62: 591–598, 1987.
13. **Levine, S., D. Silage, D. Henson, J. Wang, J. Krieg, J. LaManca, and S. Levy.** Use of a triaxial magnetometer for respiratory measurements. *J. Appl. Physiol.* 70: 2311–2321, 1991.
14. **Loring, S. H., and E. N. Bruce.** Methods for study of the chest wall. In: *Handbook of Physiology. The Respiratory System. Mechanics of Breathing.* Bethesda, MD: Am. Physiol. Soc., 1986, sect. 3, vol. III, pt. 2, chapt. 24, p. 415–428.
15. **Mouchnino, L., R. Aurenty, J. Massion, and A. Pedotti.** Coordination between equilibrium and head-trunk orientation during leg movement: a new strategy built up by training. *J. Neurophysiol.* 67: 1587–1598, 1992.
16. **Peacock, A. J., M. D. L. Morgan, S. Gourlay, C. Tourton, and D. M. Denison.** Optical mapping of the thoraco-abdominal wall. *Thorax* 39: 93–100, 1984.
17. **Pedotti, A., and G. Ferrigno.** Opto-electronics based systems. In: *Three-Dimensional Analysis of Human Movement*, edited by P. Allard, I. A. F. Stokes, and J. P. Bianchi. Champaign, IL: Human Kinetics, 1995, chapt. 4, p. 57–78.
18. **Sackner, M. A., H. Watson, A. S. Belsito, D. Feinerman, M. Suarez, G. Gonzalez, F. Bizousky, and B. Krieger.** Calibration of respiratory inductance plethysmography during natural breathing. *J. Appl. Physiol.* 66: 410–420, 1989.
19. **Ward, M. E., J. W. Ward, and P. T. Macklem.** Analysis of human chest wall motion using a two-compartment rib cage model. *J. Appl. Physiol.* 72: 1338–1347, 1992.
20. **Zimmerman, P. V., S. J. Connellan, H. C. Middleton, M. V. Tabona, M. D. Goldman, and N. Price.** Postural changes in rib cage and abdominal volume-motion coefficients and their effect on the calibration of a respiratory-inductive plethysmograph. *Am. Rev. Respir. Dis.* 127: 209–214, 1983.